

# Oxygen, $\alpha$ -element and iron abundance distributions in the inner part of the Galactic thin disc <sup>\*</sup> †

R.P. Martin<sup>1‡</sup>, S.M. Andrievsky<sup>2,3</sup>, V.V. Kovtyukh<sup>2</sup>, S.A. Korotin<sup>2</sup>, I.A. Yegorova<sup>4</sup>, and Ivo Saviane<sup>4</sup>,

<sup>1</sup>*Department of Physics and Astronomy, University of Hawai'i at Hilo, Hilo, HI, 96720, USA*

<sup>2</sup>*Department of Astronomy and Astronomical Observatory, Odessa National University and Isaac Newton Institute of Chile, Odessa Branch, Shevchenko Park, 65014 Odessa, Ukraine*

<sup>3</sup>*GEPI, Observatoire de Paris-Meudon, CNRS, Université Paris Diderot, 92125 Meudon Cedex, France*

<sup>4</sup>*European Southern Observatory, Alonso de Cordova 3107, Santiago, Chile*

Accepted, 12 March 2015. Received, 12 March 2015; in original form, 18 January 2015

## ABSTRACT

We derived elemental abundances in 27 Cepheids, the great majority situated within a zone of Galactocentric distances ranging from 5 to 7 kpc. One star of our sample, SU Sct, has a Galactocentric distance of about 3 kpc, and thus falls in a poorly investigated region of the inner thin disc. Our new results, combined with data on abundances in the very central part of our Galaxy taken from literature, show that iron, magnesium, silicon, sulfur, calcium and titanium LTE abundance radial distributions, as well as NLTE distribution of oxygen reveal a plateau-like structure or even positive abundance gradient in the region extending from the Galactic center to about 5 kpc.

**Key words:** stars: abundances – stars: Cepheids – Galaxy: evolution

## 1 INTRODUCTION

In our series of papers (Andrievsky et al. 2002a, Andrievsky et al. 2002b, Andrievsky et al. 2002c, Andrievsky et al. 2004, Luck et al. 2003, Luck et al. 2006, Luck et al. 2011) we presented the radial elemental distributions over a wide interval of Galactocentric distances based on high-resolution spectroscopic data of a large sample of Cepheids (thin disc population). Indeed, we succeeded in covering more than 10 kpc in radial direction from about 4 to 16 kpc. A gradual increase of elemental abundance as distance decreases was confirmed for many chemical elements. In particular, Andrievsky et al. (2002b) used a limited number of Cepheid stars to find the properties of the metallicity distribution in the inner part of the Galactic disc. The number of studied stars with Galactocentric distances less than 6 kpc at that time was only five, but almost all chemical elements investigated in

those stars showed clearly increased abundances comparing to the Cepheids from the solar vicinity ( $R_{\odot} \approx 8.0$  kpc).

Recently Genovali et al. (2013) presented probably the most comprehensive compilation of data on metallicity distribution obtained from Cepheids in the Galactic inner disc (with Galactocentric distances  $\geq 4.6$  kpc). That paper contains the corresponding references on relevant studies, and will not be repeated here.

The increased sophistication of observing techniques in the recent decade allows us to obtain high-resolution stellar spectra near the very center of our Galaxy. This is often achieved by using the far- and near-IR domains of the electromagnetic spectrum where absorption is much less than in the visual region. Ryde & Schultheis (2015) summarize all the results for Galactic center abundances obtained up to now.

The general picture of the metallicity distribution in the inner part of the Galactic disc can be drawn from all of these studies: the metallicity of the thin disc gradually increases toward the Galactic center, and reaches about  $[\text{Fe}/\text{H}] \approx +0.5$  at  $R_G \approx 4$  kpc. The region of the thin disc between this distance and the immediate Galactic center still remains poorly sampled, and the spatial properties of the metallicity distribution in this domain are not known. Filling in this gap would have a certain interest for the Galactic chemical evolution models.

In this paper we present abundances for stars which are

\* Based on observations obtained at the Canada-France-Hawaii Telescope (CFHT), which is operated by the National Research Council of Canada, the Institut National des Sciences de l'Univers of the Centre National de la Recherche Scientifique of France, and the University of Hawaii.

† Based on observations made with ESO Telescopes at the La Silla and Paranal Observatories under programmes 089.D0489 and 60A-9700.

‡ E-mail: rpm33@hawaii.edu

mainly situated in the region 5-7 kpc, with one Cepheid located in the critical region at about 3 kpc. Observational details are given in the next Section. Stellar atmosphere parameters relevant to our study are briefly discussed in Section 3. Abundance measurements and their radial distribution are presented in Section 4 and 5, respectively. Section 6 summarizes our results and conclusions.

## 2 OBSERVATIONS AND DATA REDUCTION

The observations were carried out with 3.6 m Canada-France-Hawaii Telescope (CFHT), the Very Large Telescope (VLT) Unit 2 Kueyen, and the 2.2 m MPG Telescope.

*CFHT.* The observations were carried out under the queue observing mode using the fiber-fed ESPaDOnS echelle spectrograph equipped with an e2v 2048 x 4608 CCD (binned 1 x 1). The resolving power provided by this combination was about 80000 and the spectral range extended from 370 to 1050 nm. The spectra were processed by the CFHT ESPaDOnS pipeline. The estimated S/N ratio at the continuum level depends upon the wavelength interval, and varies for each star in the range from about 80 to 100.

*VLT.* For data obtained with the VLT (observing run 089.D-0489), the red arm of the UVES cross-dispersed echelle spectrograph was used. With the red arm, the wavelength region between 420 nm and 1100 nm can be scanned. The grating angle was set at 22.668 degrees thus allowing to cover a wavelength interval between 479 nm and 681 nm. The light is dispersed over two CCD chips, with a gap between 576 nm and 583 nm. The slit was set at 1'' width and 12'' length, yielding a resolution of 38700. The median SNR for the upper and lower chip spectra are  $\approx 50$  and  $\approx 14$ , respectively but with a relatively large range: from  $\approx 32$  to  $\approx 56$  for the upper, and from  $\approx 11$  to  $\approx 40$  for the lower chip.

*ESO/MPGT.* For data taken with the ESO/MPG 2.2 m telescope, the FEROS spectrograph was used (Kaufer et al. 1999). The instrument has a wavelength coverage from  $\approx 350$  nm to  $\approx 920$  nm, and a resolving power of 48000. The typical SNR ratio of our spectra is  $\approx 90$ . Each night a broad-line B star was observed with a SNR exceeding that of the program stars, in order to enable cancellation of the telluric lines when necessary.

Table 1 contains details on our observations of Cepheids for this study, as well as some information about the physical properties of the Cepheids themselves (see next Section).

The processing of spectra (continuum level determination, equivalent widths measurements etc.) was carried out by using the DECH20 software package (Galazutdinov 1992). The line-list is the same as used in our previous studies (see Kovtyukh & Andrievsky 1999).

## 3 STELLAR ATMOSPHERE PARAMETERS

The effective temperature ( $T_{\text{eff}}$ ) for the stars in our program was estimated by calibrating the ratios of the central depths of the lines with different potentials of the lower levels (see Kovtyukh 2007). The surface gravity values were computed using the iron ionization balance. The microturbulent velocity was found by avoiding any dependence between the iron abundance as produced by individual Fe II lines and their

equivalent widths. The resulting atmosphere parameters for the studied stars are listed in Table 1.

## 4 SPECTROSCOPIC ANALYSIS

All abundances listed in Tables 2 and 3 (with an exception for oxygen, sulfur and barium) were derived in the LTE approximation in order to be consistent with our previous abundance determinations in Cepheids. For this we used the ATLAS9 code (Kurucz 1992) to generate the appropriate atmosphere models, and Kurucz's WIDTH9 code to analyze the equivalent widths. The reference solar abundances were taken from Grevesse & Sauval (1998).

Expected errors in abundances caused by variations in the fundamental stellar parameters are presented in Table 4 for our critical object SU Sct. The total abundance error was obtained by increasing the temperature by 100 K, surface gravity by 0.2 dex and microturbulent velocity by 0.5  $\text{km s}^{-1}$ . Decreasing these parameters by similar values will produce almost the same errors.

Our sample includes several stars in common with the studies of Genovali et al. (2014) and Luck & Lambert (2011). In Table 5 we compare our iron abundance measurements with those of the above studies. Generally, there is reasonable agreement between these independent results.

An exception in this paper was made for oxygen and barium whose NLTE abundances for a large sample of Cepheids were previously derived by us (Luck et al. 2013, Korotin et al. 2014, Andrievsky et al. 2013, Andrievsky, Luck & Korotin 2014). In those papers the reader can find all the details concerning the method of the NLTE calculations and applied atomic models of oxygen and barium. For sulfur we present both LTE and NLTE abundances. The NLTE sulfur atomic model used for the NLTE analysis was described by Korotin (2009).

In the next section we present the radial abundance distributions for some chemical elements. The distances for the stars of the present sample were found in the same way as in Andrievsky et al. (2002a). For three stars of our program the E(B-V) values, which are necessary to estimate the heliocentric distances, are not available in the literature (the stars V5567 Sgr, ASAS 171305-4323, and BD-04 4569). Therefore they were derived by us using the correlation between the diffuse interstellar band (DIB) equivalent widths measured in their spectra and E(B-V) indices as proposed by Friedman et al. (2011). For this we used the interstellar features at 5780.5, 5797.1 and 6613.6 Å. To remove the stellar lines from the DIB region before the equivalent width measurement, we used a synthetic spectrum technique. The accuracy of the E(B-V) values determined by this method is approximately 10-15%.

For the star SU Sct, which has the smallest Galactocentric distance in our sample, we compared our estimate of the E(B-V) to the literature value provided by Ngeow (2012), who applied the Wesenheit function in deriving distances to Galactic Cepheids. According to this method, the heliocentric distance of SU Sct is 6.62 kpc, that gives  $R_G = 3.04$  kpc, in good agreement with our value listed in Table 1.

**Table 1.** Observations and parameters of the investigated stars

Star	P, d	JD(start) 245..	V	E(B-V)	Telescope	$T_{\text{eff}}$ , K	$\log g$	$V_t$ , km s $^{-1}$	$R_G$ , kpc
V340 Ara	20.8090000	4186.72337651	10.164	0.546	MPGT	5318	1.15	4.2	4.34
SS CMa	12.3610001	6289.79272864	9.915	0.549	MPGT	5380	1.50	4.5	9.71
TV CMA	4.6700101	6289.78263332	10.582	0.583	MPGT	5754	2.10	3.7	9.56
AG Cru	3.83728	5966.84795300	8.225	0.212	MPGT	5730	2.15	4.6	7.35
X Cru	6.2199702	5966.87123636	8.404	0.272	MPGT	5394	1.70	4.5	7.20
V1033 Cyg	4.9375119	6524.95738426	13.027	1.067	CFHT	5819	2.10	3.4	7.46
EK Pup	2.6259401	6289.79920932	10.664	0.328	MPGT	6434	2.30	4.0	9.73
WY Pup	5.2508001	6289.82627777	10.569	0.270	MPGT	6537	2.30	5.0	10.26
KQ Sco	28.6896000	6141.67867798	9.807	0.869	MPGT	5697	2.00	6.2	5.41
V470 Sco	16.2614994	6518.72862269	11.069	1.517	CFHT	5906	1.70	4.9	6.62
X Sct	4.1980700	6524.80085648	10.006	0.619	CFHT	5811	2.15	4.7	6.46
Y Sct	10.3414831	6524.81630787	9.628	0.823	CFHT	5145	1.60	3.8	6.55
		6092.89682642			VLT	5643	2.00	6.0	
BX Sct	6.4113302	6524.86835648	12.241	1.318	CFHT	5599	2.00	3.6	6.38
CK Sct	7.4152198	6518.82194444	10.590	0.795	CFHT	5735	2.00	4.3	6.13
CM Sct	3.9169769	6518.87042824	11.106	0.771	CFHT	5679	2.00	3.6	6.23
CN Sct	9.9923000	6524.83060185	12.478	1.267	CFHT	5456	1.80	5.0	5.64
RU Sct	19.7006207	6524.82368056	9.466	0.957	CFHT	5180	1.50	4.7	6.52
SU Sct	1.4679780	6524.88760417	13.663	0.459	CFHT	5975	2.80	3.3	3.22
		6069.88148484			VLT	6190	2.60	4.5	
TY Sct	11.05302	6518.85549769	10.831	1.014	CFHT	5487	1.90	5.5	6.16
		6092.90857267			VLT	5811	1.80	4.8	
AA Ser	17.1411991	6518.83685185	12.228	1.603	CFHT	5388	1.50	4.2	6.30
CR Ser	5.3014102	6524.78538194	10.842	1.011	CFHT	6169	2.15	4.2	6.57
AY Sgr	6.5695901	6518.80657407	10.549	0.919	CFHT	5714	1.90	3.7	6.36
V773 Sgr	5.7484450	6524.74738426	12.389	1.620	CFHT	5467	1.50	3.9	6.73
V1954 Sgr	6.1794491	6518.79149306	10.831	0.875	CFHT	5501	1.80	3.8	6.07
V5567 Sgr	9.7616	6147.73398282	10.550	0.990	VLT	5868	2.00	4.7	6.26
ASAS 171305-4323	9.555323	6124.72436291	12.645	1.630	VLT	6153	2.40	5.4	5.96
BD -04 4569	13.83873	6124.81107798	10.026	1.300	VLT	5620	2.30	7.0	7.00

Remark: Reddening values are from Fouqué et al. (2007) or Fernie et al. (1995) with the systematic correction of Fouqué et al. (2007) applied (factor 0.952). These reddening values are on the E(B-V) scale by Laney et al. (2007). Note that for some stars the reddening values were found using a special method (see Sect. 4).

## 5 RESULTS AND DISCUSSION

In Fig. 1 we show the iron abundance distribution of Galactic Cepheids from our previous studies and the present sample together with the Galactic center abundances. The Cepheids of our program cover a similar pulsation period range as the stars included in our previous samples; thus they share a similar age range. Following the period-age relation for classical Cepheids as proposed by Bono et al. (2005), the age range of the Cepheids in our sample is roughly 20-70 Myr. The average iron abundance at the Galactic Center from literature presented in Fig. 1 was mostly determined from stars covering a larger age range, that is from members of the Arches/Quintuplet clusters ( $\sim 3$ -9 Myr) to field stars of  $\sim 1$ Gyr. For iron and other elements, the absolute abundances derived by other authors were normalized to the solar abundances from Grevesse & Sauval (1998).

As explained earlier, one of our stars (SU Sct) in the critical region between the central part and 5 kpc gives some reason to believe that the iron content in the Galactic thin disc young population stars (in Cepheids, in particular) does not exceed the value of about +0.4 dex if we use our homogeneous data, or +0.5 when using the compilation data of Genovali et al. (2013). After reaching the value of  $[\text{Fe}/\text{H}] = +0.4$  dex at about 5 kpc the metallicity tends to slightly decrease in the direction of the Galactic center.

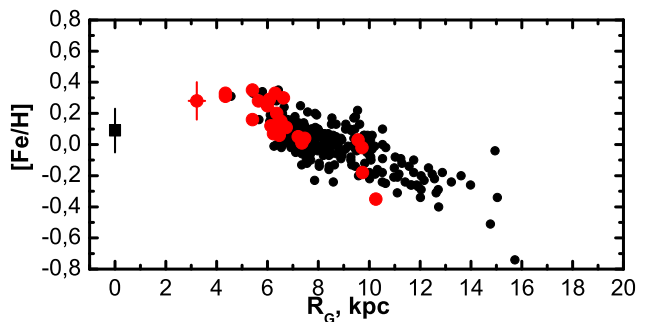


**Figure 1.** LTE iron abundance distribution in Galactic disc. Black circles - our previous determinations published in a series of papers mentioned in the Introduction. Red circles - present sample. For SU Sct we show the typical for Cepheids the iron abundance uncertainty ( $2\sigma$ ), and 10% uncertainty in the distance. The Galactic center iron abundance is a mean value calculated from the individual star abundances published by Carr et al. (2000), Ramirez et al. (2000), Cunha et al. (2007), Davies et al. (2009) and Ryde & Schultheis (2015). The  $2\sigma$  interval is showed for this data point.

Similar trends can also be seen for such elements as magnesium, silicon, sulfur, calcium and titanium, whose abundances in the Galactic center nowadays are known (Fig.

**Table 2.** The abundances of the investigated stars (C–Mn)

Star	C	N	O	Na	Mg	Al	Si	S	S <sub>LTE</sub>	Ca	Sc	Ti	V	Cr	Mn
V340 Ara	0.23	0.89	0.36	0.55	0.21	0.40	0.31	0.30	0.48	0.16	0.30	0.23	0.21	0.30	0.30
SS CMa–0.19	0.68	–0.01	0.17	–0.18	0.05	–0.03	0.03	–0.13	–0.20	–0.16	–0.06	–0.12	–0.14	–0.14	–0.16
TV CMa–0.17	0.46	–0.08	0.14	–0.03	–0.01	0.06	–0.02	0.12	–0.12	0.02	0.00	–0.03	–0.04	–0.04	–0.15
AG Cru–0.14	0.53	–0.04	0.20	–0.09	0.08	0.02	–0.01	0.12	–0.07	–0.03	–0.02	–0.03	–0.01	–0.01	–0.11
X Cru–0.05	0.18	0.06	0.24	–0.19	0.10	0.05	0.09	0.15	–0.03	–0.05	–0.04	–0.06	–0.04	–0.04	–0.02
V1033 Cyg	0.05	–0.09	0.01	–0.17	–0.05	0.04	0.06	0.02	0.16	0.03	0.02	0.05	–0.02	–0.01	–0.13
EK Pup–0.41	0.31	–0.15	–0.09	–0.26	–0.20	–0.07	–0.18	–0.16	–0.29	–0.19	–0.21	–0.14	–0.27	–0.27	–0.28
WY Pup–0.42	–0.09	–0.17	–0.20	–0.27	...	–0.16	–0.28	–0.29	–0.38	–0.41	–0.37	–0.21	–0.41	–0.41	–0.37
KQ Sco	0.10	0.71	0.36	0.44	0.34	0.26	0.26	0.30	0.40	0.17	0.35	0.27	0.29	0.36	0.27
V470 Sco	0.12	0.66	0.18	0.57	0.26	0.34	0.30	0.15	0.45	0.26	0.33	0.32	0.30	0.31	0.22
X Sct–0.08	0.35	–0.02	0.24	0.00	0.05	0.04	–0.01	0.11	0.20	0.04	0.10	0.05	0.10	0.10	–0.11
Y Sct–0.12	0.75	0.25	0.28	–0.03	0.15	0.10	0.16	0.16	0.10	0.11	0.08	0.05	0.08	0.08	0.04
BX Sct–0.07	0.43	0.12	0.24	0.01	0.14	0.10	0.14	0.23	0.11	0.09	0.10	0.03	0.05	0.05	–0.01
CK Sct–0.02	0.41	0.15	0.15	–0.06	0.07	0.10	0.14	0.22	0.10	0.12	0.13	0.04	0.07	0.07	–0.06
CM Sct–0.16	0.28	0.13	0.22	–0.02	0.04	0.07	–0.01	0.13	0.07	0.07	0.03	0.02	0.04	0.04	–0.08
CN Sct	0.20	0.77	0.29	0.38	0.35	0.20	0.28	0.25	0.44	0.14	...	0.23	0.20	0.13	0.15
RU Sct	0.06	0.66	0.15	0.20	–0.09	0.09	0.10	0.16	0.30	0.05	0.08	0.02	0.01	0.04	0.04
SU Sct	0.31	0.62	0.35	0.10	0.19	–0.04	0.17	0.29	0.36	–0.01	0.11	0.09	0.40	0.26	0.22
TY Sct	0.18	0.60	0.29	0.40	0.16	0.26	0.21	0.27	0.39	0.18	0.30	0.23	0.23	0.15	0.15
AA Ser	0.31	0.90	0.40	0.48	0.27	0.34	0.30	0.34	0.58	0.32	0.35	0.18	0.28	0.33	0.25
CR Ser–0.18	0.53	0.07	0.26	0.12	0.08	0.14	0.04	0.04	0.24	0.02	0.07	0.12	0.10	0.13	–0.01
AY Sgr–0.01	0.45	0.18	0.35	0.18	0.18	0.18	0.18	0.16	0.32	0.15	0.17	0.12	0.12	0.16	0.10
V773 Sgr–0.13	0.32	0.02	0.29	0.11	0.19	0.18	0.01	0.18	0.17	0.02	0.13	0.07	0.10	0.10	0.12
V1954 Sgr	0.13	0.65	0.16	0.56	0.19	0.32	0.30	0.20	0.43	0.25	0.23	0.21	0.21	0.26	0.28
V5567 Sgr–0.17	...	0.18	0.19	–0.16	0.09	0.05	...	0.08	0.03	0.06	0.07	0.01	0.05	0.05	–0.11
ASAS 171305–4323	0.10	...	0.24	0.51	0.11	0.26	0.28	...	0.41	0.31	0.46	0.29	0.32	0.34	0.20
BD-04 4569	0.04	...	...	0.05	...	0.15	0.03	...	0.14	0.02	...	0.10	0.25	0.28	–0.01

**Table 3.** The abundances of the investigated stars (Fe–Gd)

Star	Fe	Co	Ni	Cu	Zn	Y	Zr	Ba	La	Ce	Pr	Nd	Sm	Eu	Gd
V340 Ara	0.32	0.18	0.35	0.28	0.36	0.32	0.21	0.17	0.18	0.00	0.09	0.03	0.43	0.28	0.23
SS CMa–0.02	–0.28	–0.12	–0.12	–0.23	–0.17	0.11	0.18	0.27	0.18	–0.01	–0.04	–0.02	...	0.01	...
TV CMa	0.03	–0.18	–0.04	–0.12	–0.29	0.20	0.22	0.20	0.14	0.15	–0.06	0.01	...	0.03	...
AG Cru	0.01	–0.22	–0.02	–0.08	0.04	0.17	–0.02	–0.15	0.17	–0.06	–0.30	–0.10	...	0.10	...
X Cru	0.05	–0.21	–0.03	–0.13	0.08	0.17	0.13	0.00	0.19	0.06	–0.24	–0.05	...	0.10	...
V1033 Cyg	0.04	0.02	0.01	–0.04	0.11	0.16	0.09	0.14	–0.03	0.12	0.05	0.09	...	0.16	...
EK Pup–0.18	–0.22	–0.21	–0.40	–0.47	–0.05	–0.02	–0.05	...	–0.13	–0.07	–0.10	...	0.06	...	...
WY Pup–0.35	...	–0.39	–0.26	–0.43	–0.22	–0.05	0.02	...	–0.04	...	0.02	...	...	...	...
KQ Sco	0.35	0.21	0.35	0.30	0.34	0.37	0.39	0.20	0.26	0.05	0.20	0.14	0.48	0.38	0.44
V470 Sco	0.30	0.26	0.32	0.13	0.19	0.36	0.37	0.09	0.29	0.09	0.08	0.18	0.17	0.28	0.32
X Sct	0.06	–0.06	0.04	0.03	0.14	0.15	0.13	0.08	0.19	0.09	0.06	0.11	0.32	0.30	0.32
Y Sct	0.13	0.00	0.10	–0.06	0.29	0.26	0.10	0.25	0.20	0.08	0.02	0.06	0.35	0.20	0.17
BX Sct	0.13	0.03	0.11	0.03	0.16	0.34	...	0.23	0.31	0.14	–0.05	0.18	...	0.20	...
CK Sct	0.12	0.01	0.09	–0.04	0.10	0.29	0.07	0.19	0.17	0.09	–0.04	0.06	...	0.14	...
CM Sct	0.07	–0.05	0.04	–0.11	0.02	0.22	0.12	0.17	–0.09	0.06	–0.07	0.05	...	0.10	...
CN Sct	0.28	0.13	0.25	0.20	...	0.37	0.13	0.20	0.28	0.18	...	0.43	...	0.29	...
RU Sct	0.15	–0.04	0.06	–0.20	0.25	0.27	0.19	0.14	0.06	0.06	0.03	0.15	0.25	0.20	0.17
SU Sct	0.27	0.44	0.20	0.29	0.05	0.15	0.32	0.25	0.49	0.48	...	0.09	...	0.34	...
TY Sct	0.25	0.18	0.30	0.17	0.39	0.30	0.34	0.18	0.18	0.08	...	0.08	...	0.32	...
AA Ser	0.33	0.18	0.35	0.29	...	0.36	0.39	0.17	0.25	0.06	0.07	0.04	0.15	0.33	0.33
CR Ser	0.11	0.05	0.10	0.04	0.09	0.27	0.20	0.14	0.07	0.21	0.09	0.18	0.10	0.22	0.24
AY Sgr	0.20	0.05	0.16	0.05	0.25	0.31	0.27	0.32	0.13	0.20	0.09	0.14	0.14	0.17	0.32
V773 Sgr	0.11	–0.01	0.13	0.04	0.16	0.15	0.14	0.12	0.17	0.02	0.03	0.16	0.38	0.21	...
V1954 Sgr	0.29	0.17	0.28	0.17	...	0.28	0.29	0.17	0.15	0.14	0.03	0.09	0.33	0.32	...
V5567 Sgr	0.07	–0.05	0.00	–0.14	–0.21	0.25	0.15	0.05	0.02	0.18	–0.13	0.06	0.03	0.18	0.05
ASAS 171305–4323	0.32	0.27	0.29	...	0.33	0.42	0.32	–0.05	0.32	0.24	0.12	0.15	0.31	0.35	0.26
BD-04 4569	0.08	...	0.08	...	...	0.18	0.36	0.05	0.45	0.22	...	0.18	...	0.41	...

2). Despite the fact that abundances of these elements were derived in LTE, we believe that the general tendency noticed for iron, and also seen for these  $\alpha$ -elements, will not change qualitatively after the applying the NLTE corrections (in particular, this conclusion is supported by our result for sulfur, where we show both LTE and NLTE abundances for the present sample of stars).

As one can see, the iron and  $\alpha$ -elements demonstrate a clear plateau in their abundance distributions, or even positive gradient value in the region from the Galactic center to about 5 kpc. This is also clearly seen in our fully NLTE abundance distribution of the oxygen (see Fig. 3). Similar to iron, the highest oxygen abundance in the thin disc is achieved at about 4-5 kpc at a value of about +0.4 dex. Figures 2 and 3 show that there is no overabundance of the oxygen and  $\alpha$ -elements with respect to iron, in agreement with what is expected for thin disc stars.

It is also interesting to note that in contrast with elements discussed above, barium, which is mainly produced by low mass AGB stars, does not display any remarkable trend with the Galactocentric distance neither in the outer or in the inner part of the Galactic disc, as shown in Fig. 4.

Bronfman et al. (1988) derived the mean radial distribution of molecular clouds in Galactic disc, and found that the highest density of interstellar gas is observed in the Galactocentric distance range of 4 to 8 kpc with a maximum value at about 5-6 kpc. At the distance of about 3-4 kpc there is an abrupt drop in the gas surface density. The same result follows from the papers of Sanders, Solomon & Scoville (1984) and Dame (1993). If a lower gas density causes a decrease in the star formation rate in the region with Galactocentric distance less than 4 kpc, then the chemical enrichment of interstellar matter from SNe will not be effective in this region. This should be imprinted on the derived abundances of the young population stars within the Galactic bar, whose influence on the chemical properties of the inner part of our Galaxy must be strong. Existing theoretical models that deal with the inner part of the Galaxy do not reproduce these observed trends in the central part (0-6 kpc) quite correctly, although some of them take into account the radial gas flow, as well as the bar influence on the chemistry of the inner disc. Nevertheless, the general improvement seen with those models seems to be clear. This is demonstrated by the oxygen and iron plots in Fig. 5.

## 6 CONCLUSIONS AND FINAL REMARKS.

We derived abundances of 29 elements in 27 Cepheids located mainly within 5-7 kpc from Galactic center, with one star SU Sct situated in a poorly sampled region of the thin disc between 4 kpc and the Galactic center. We found that in the inner region of our Galaxy the abundance distributions of oxygen, some  $\alpha$ -elements and iron show a plateau-like structure, or even positive slope. Despite the small number of data points within 4 kpc, this finding may have significant impact on the Galactic chemical evolution models that include the Galactic bar, and its influence on radial gas flows. Future observing programs aiming at obtaining additional high-resolution spectra of faint Cepheids located within the 0 - 4 kpc zone in the Galaxy disc would be very valuable.

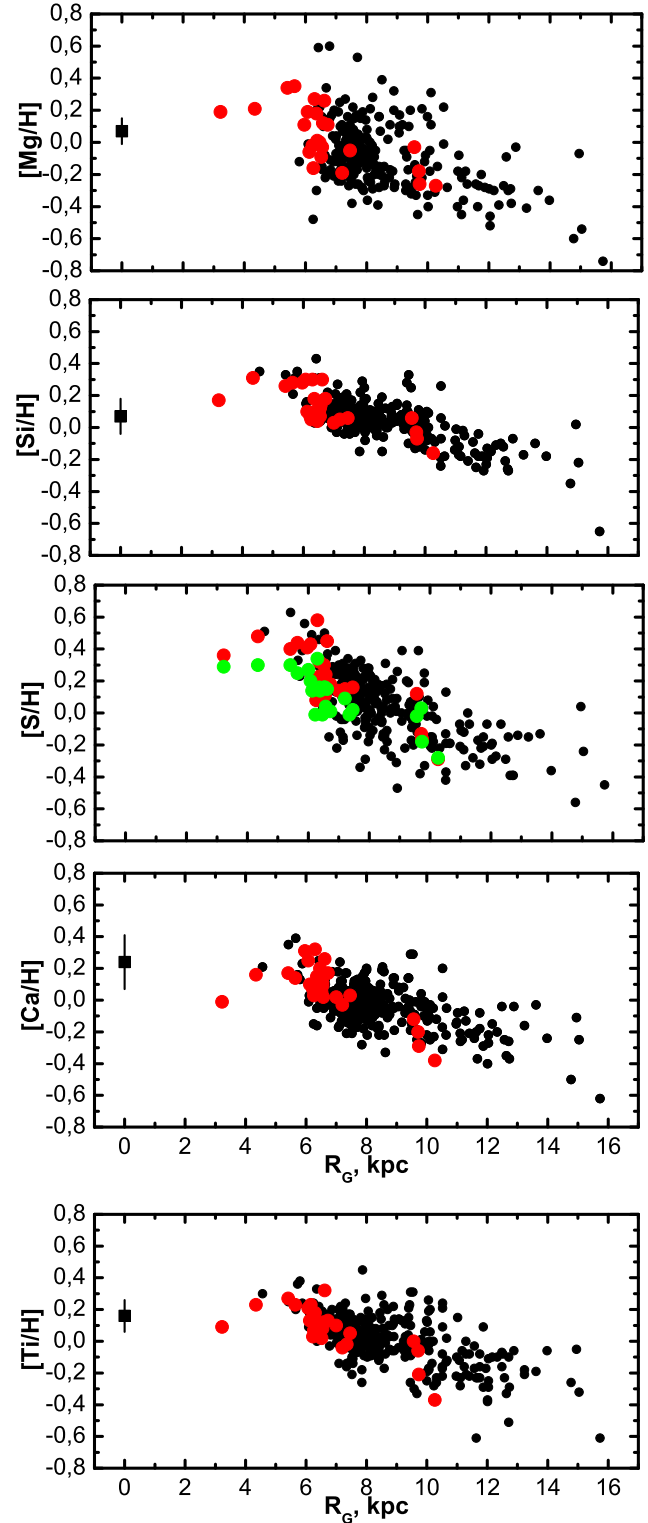


**Figure 2.** The same as Fig.1 but for magnesium, silicon, sulfur, calcium and titanium. Green circles in the sulfur plot - our NLTE abundances for the stars of present sample. The Galactic center abundance data are from Cunha et al. (2007), Davies et al. (2009) and Ryde & Schultheis (2015). The Galactic center abundance of sulfur is not available, but we show this element together with other  $\alpha$ -element abundance distributions.

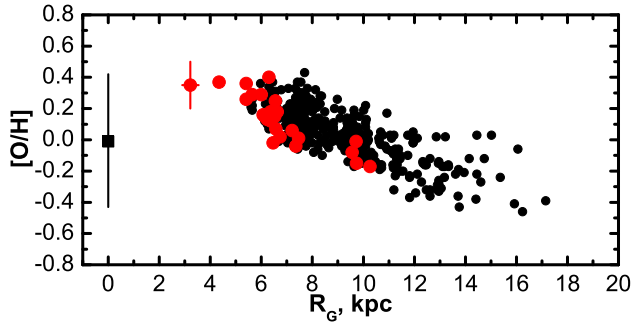


**Figure 3.** The NLTE abundance distribution of oxygen vs. Galactocentric distance. Black circles - Luck et al. (2013) and Korotin et al. (2014), red circles - present sample of Cepheids. The Galactic center abundance is the mean value based on the data from Carr et al. (2000), Cunha et al. (2007) and Davies et al. (2009).

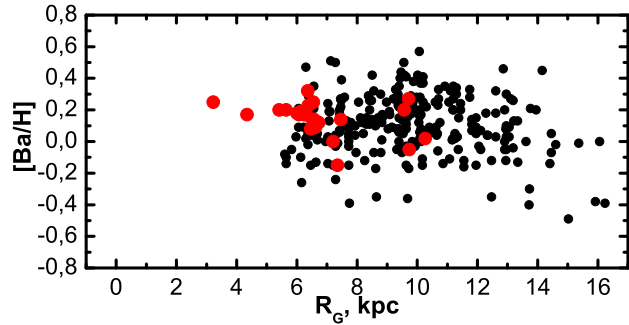


**Figure 4.** The NLTE abundance distribution of barium vs. Galactocentric distance. Black circles - Andrievsky et al. (2013), Andrievsky, Luck & Korotin (2014), red circles - present sample of Cepheids. The Galactic center abundance of this element is not available.

## ACKNOWLEDGMENTS

SMA and SAK acknowledge the SCOPES grant No. IZ73Z0-152485 for financial support. We acknowledge the queue observing team at CFHT and support staff at the VLT and MPGT, and also J.R.D. Lépine for his valuable comments. Authors are thankful to the anonymous referee for her/his comments.

## REFERENCES

Andrievsky, S.M., Kovtyukh, V.V., Luck, R.E., Lépine J.R.D., Bersier D., Maciel W.J., Barbuy B., Klochkova V.G., Panchuk V.E., & Karpischeck R.U., 2002a, *A&A*, 381, 32  
 Andrievsky, S.M., Bersier, D., Kovtyukh, V.V., Luck R.E., Maciel W.J., Lépine J.R.D., & Beletsky Yu.V., 2002b, *A&A*, 384, 140  
 Andrievsky, S.M., Kovtyukh, V.V., Luck, R.E., Lépine, J.R.D., Maciel, W.J., & Beletsky, Yu.V., 2002c, *A&A*, 392, 491  
 Andrievsky, S.M., Luck, R.E., Martin, P., & Lépine, J.R.D., 2004, *A&A*, 413, 159  
 Andrievsky, S.M., Lépine, J.R.D., Korotin, S.A., Luck,

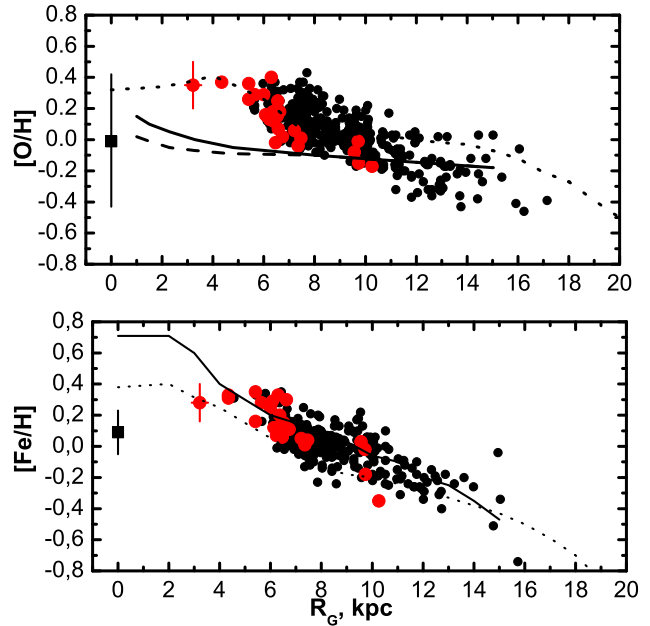


**Figure 5.** Our abundance distributions of oxygen and iron superimposed with theoretical curves for oxygen from Cavichia et al. (2014) - dotted line, and Fu et al. (2013) - the model with radial gas inflow - solid line, and without it - dashed line, and for iron from Cavichia et al. (2014) - dotted line, and Minchev et al. (2013) - solid line. Note that we re-scaled the absolute oxygen abundances of Cavichia et al. (2014) assuming that their “solar” oxygen abundance (i.e. abundance at  $R_G \approx 8$  kpc)  $12+\log(O/H) = 8.4$ .

R.E., Kovtyukh, V.V., & Maciel, W.J., 2013, *MNRAS*, 428, 3252  
 Andrievsky, S.M., Luck, R.E., & Korotin, S.A., 2014, *MNRAS*, 437, 2106  
 Bronfman, L., Cohen, R.S., Alvarez, H., May, J., & Thaddeus, P., 1988, *ApJ*, 324, 248  
 Bono, G., Marconi, M., Cassisi, S., Caputo, F., Gieren, W., Pietrzynski, G., 2005, *ApJ*, 621, 966  
 Carr, J.S., Sellgren, K., & Balachandran, S.C., 2000, *ApJ*, 530, 307  
 Cavichia O., Mollá M., Costa R.D.D., & Maciel W.J., 2014, *MNRAS* 437, 3688  
 Cunha, K., Sellgren, K., Smith, V.V., Ramirez, S.V., Blum, R.D., & Terndrup, D.M., 2007, *ApJ* 669, 1011  
 Dame, T.M., 1993, *Back to the Galaxy*, Eds. S.S. Holt, F. Verter, *AIP Conf. Proc.* 278, 267  
 Davies, B., Origlia, L., Kudritzki, R.-P., Figer, D.F., Rich, R.M., & Najarro, F., 2009, *ApJ*, 694, 46  
 Fernie, J. D., Evans, N. R., Beattie, B., Seager, S., 1995, *IBVS* 4148, 1  
 Fouqué, P., Arriagada, P., Storm, J., Barnes, T.G., Nardetto, N., Mérand, A., Kervella, P., Gieren, W., Bersier, D., Benedict, G.F., McArthur, B.E., 2007, *A&A* 476, 73  
 Friedman, S.D., York, D.G., McCall, B.J., Dahlstrom, J., Sonnentrucker, P., Welty, D.E., Drosback, M.M., Hobbs, L.M., Rachford, B.L., & Snow, Th.P., 2011, *ApJ*, 727, 33  
 Fu, J., Kauffmann, G., Huang Mei-ling, Yates, R.M., Moran, S., Heckman, T.M., Dave, R., Guo, Q., & Hen-

**Table 4.** Abundance uncertainties due to stellar atmospheric parameters. SU Sct (VLT,  $T_{\text{eff}}=6190$  K,  $\log g=2.6$ ,  $V_t=4.5$  km s $^{-1}$ ,  $[\text{Fe}/\text{H}] = +0.26$ ).

Species	$\Delta T_{\text{eff}}$ +100 K	$\Delta \log g$ +0.2	$\Delta V_t$ +0.5 km s $^{-1}$	Total error
6.00	-0.05	0.06	-0.02	0.08
11.00	0.05	-0.01	-0.03	0.06
12.00	0.05	-0.01	-0.03	0.06
13.00	0.05	-0.01	-0.01	0.05
14.00	0.04	-0.01	-0.02	0.05
14.01	-0.08	0.06	-0.02	0.10
16.00	-0.03	0.04	-0.03	0.06
20.00	0.06	-0.01	-0.04	0.07
21.01	0.02	0.08	-0.04	0.09
22.00	0.08	-0.01	-0.01	0.08
22.01	0.02	0.08	-0.05	0.10
23.00	0.09	-0.02	-0.01	0.09
23.01	0.02	0.08	-0.01	0.08
24.00	0.07	-0.01	-0.01	0.07
24.01	-0.01	0.08	-0.05	0.09
25.00	0.07	-0.01	-0.02	0.07
26.00	0.07	-0.01	-0.02	0.07
26.01	-0.01	0.07	-0.05	0.09
27.00	0.07	-0.02	-0.01	0.07
28.00	0.07	-0.01	-0.02	0.07
29.00	0.08	-0.02	-0.03	0.09
30.00	0.07	0.00	-0.05	0.09
39.01	0.03	0.07	-0.02	0.08
40.01	0.03	0.07	-0.01	0.08
57.01	0.04	0.07	-0.01	0.08
58.01	0.04	0.07	-0.01	0.08
60.01	0.05	0.07	0.00	0.09
63.01	0.03	0.07	-0.02	0.08

**Table 5.** Comparison of the iron abundance results.

Star	This paper	GET	LL
V340 Ara	0.32	0.33± 0.09	
SS CMa	-0.02		0.07
TV CMa	0.03		0.14
X Cru	0.05		0.15
AG Cru	0.01		0.08
V1033 Cyg	0.04		0.12
KQ Sco	0.35	0.52± 0.08	
Y Sct	0.13		0.23
BX Sct	0.13		0.28
CK Sct	0.12		0.21
CM Sct	0.07		0.15
CN Sct	0.28		0.33
RU Sct	0.15	0.14± 0.04	0.11
TY Sct	0.25		0.37
AA Ser	0.33		0.41

Remark: GET - Genovali et al. (2014); LL - Luck & Lambert (2011)

riques, B.M.B., 2013, MNRAS, 434, 1531  
 Galazutdinov, G. A., 1992, Preprint SAO RAS, No. 92  
 Genovali, K. et al., 2013, A&A, 554, 132  
 Genovali, K. et al., 2014, A&A, 566, 37  
 Grevesse, N., & Sauval, A.J., 1998, Space Sci. Rev. 85, 161  
 Kaufer, A., Stahl, O., Tubbesing, S., Norregaard, P., Avila,

G., Francois, P., Pasquini, L., Pizzella, A., 1999, The Messenger, 95, 8  
 Korotin, S.A., 2009, AZh, 53, 651  
 Korotin, S.A., Andrievsky, S.M., Luck, R.E., Lépine, J.R.D., Maciel, W.J., & Kovtyukh, V.V., 2014, MNRAS, 444, 3301  
 Kovtyukh, V.V., 2007, MNRAS, 378, 617  
 Kovtyukh, V.V., & Andrievsky, S.M., 1999, A&A, 351, 597  
 Kurucz, R. L. 1992, in The Stellar Populations of Galaxies, ed. B. Barbuy, & A. Renzini, IAU Symp. 149, 225  
 Laney, C. David, Caldwell, John A. R., 2007, MNRAS 377, 147  
 Luck, R.E., Gieren, W.P., Andrievsky, S.M., Kovtyukh V.V., Fouqué P., Pont F., Kienzle F., 2003, A&A, 401, 939  
 Luck, R.E., Kovtyukh, V.V., & Andrievsky, S.M., 2006, AJ, 132, 902  
 Luck, R.E., Andrievsky, S.M., Kovtyukh, V.V., Gieren, W., & Graczyk, D., 2011, AJ, 142, 51  
 Luck, R.E., Lambert, D.L., 2011, AJ 142, 13  
 Luck, R.E., Andrievsky, S.M., Korotin, S.N., & Kovtyukh, V.V., 2013, AJ, 146, 18  
 Minchev, I., Chiappini, C., & Martig, M., 2013, A&A, 558, 9  
 Ngeow, Chow-Choong, 2012, ApJ, 747, 50  
 Ramirez, S.V., Sellgren, K., Carr, J.S., Balachandran, S.C., Blum, R., Terndrup, D.M., & Steed, A., 2000, ApJ, 537, 205  
 Ryde, N., & Schultheis, M., 2015, A&A, 573, 14  
 Sanders, D.B., Solomon, P.M., & Scoville, N.Z., 1984, ApJ, 276, 182

This paper has been typeset from a  $\text{\TeX}$ / $\text{\LaTeX}$  file prepared by the author.